Impaired megakaryopoiesis and behavioral defects in *mafG*-null mutant mice

Jordan A. Shavit,[1,3] Hozumi Motohashi,[2,3] Ko Onodera,[1,3] Jun-etsu Akasaka,[2] Masayuki Yamamoto,[2] and James Douglas Engel[1,4]

[1]Department of Biochemistry, Molecular Biology, and Cell Biology, Northwestern University, Evanston, Illinois 60208-3500 USA; [2]Institute of Basic Medical Sciences and Center for TARA, University of Tsukuba, Tsukuba 305, Japan

The small Maf proteins (MafG, MafK, and MafF), which serve as heterodimeric partner molecules of CNC family proteins for binding in vitro to MARE sites, have been implicated in the regulation of both transcription and chromatin structure, but there is no current evidence that the proteins fulfill these functions in vivo. To elucidate possible contributions of the small Maf proteins to gene regulation, we have ablated the *mafG* and *mafK* genes in mice by replacing their entire coding sequences with the *Escherichia coli lacZ* gene. *mafG* homozygous mutant animals exhibit impaired platelet formation accompanied by megakaryocyte proliferation, as well as behavioral abnormalities, whereas *mafK*-null mutant mice are phenotypically normal. Characterization of the *mafG* and *mafK* embryonic expression patterns show that their developmental programs are distinct and intersecting, but not entirely overlapping. These results provide direct evidence that the small Maf transcription factors are vital participants in embryonic development and cellular differentiation.

[*Key Words:* Small Maf proteins; gene knockouts; thrombocytopenia; neuronal deficit]

Received April 20, 1998; revised version accepted May 21, 1998.

The product of the *maf* proto-oncogene and its related family members (the Maf family proteins) share well conserved basic and leucine zipper (bZip) motifs that mediate DNA binding and dimer formation. Members of the Maf family are divided into two subfamilies: the large Maf proteins, c-Maf (Nishizawa et al. 1989), MafB (Kataoka et al. 1994a), and NRL (Swaroop et al. 1992), all of which contain a distinctive acidic domain that enables transcriptional activation, and the small Maf proteins, MafK (Fujiwara et al. 1993), MafF (Fujiwara et al. 1993) and MafG (Kataoka et al. 1995), which appear to consist of little more than the essential regions required for DNA binding and heptad repeat interactions.

Transcription factor NF-E2 is composed of two subunits, p45 and p18 (Andrews et al. 1993a,b; Igarashi et al. 1994), where the p18 subunit was shown to be a small Maf protein (for reviews, see Blank and Andrews 1997; Motohashi et al. 1997). Heterodimers of p45 and small Mafs can activate transcription from MAREs [Maf recognition elements, TGCTGAC(T/GT)CAGCA], whereas small Maf homodimers form active repressors acting on the same sites (Nagai et al. 1998). Adding to this regulatory complexity, p45 was subsequently identified as only one member of a larger group of proteins that now constitute the mammalian cap'n'collar (CNC; Mohler et al. 1991) protein family—these are called p45, Nrf1 (/LCRF1/TCF11), Nrf2 (/ECH), Bach1, and Bach2 (Chan et al. 1993; Caterina et al. 1994; Luna et al. 1994; Moi et al. 1994; Itoh et al. 1995; Oyake et al. 1996). These five CNC family members display similar heterodimeric interactions, but also include unique differences in transactivation potential in association with the small Maf proteins (Itoh et al. 1995; Johnsen et al. 1996; Oyake et al. 1996). As noted originally, the MARE also encompasses a consensus AP-1 binding site (Engel 1994). It has been shown that the small Maf proteins can interact with c-Fos, whereas the large Mafs can heterodimerize with c-Fos and/or c-Jun (Kataoka et al. 1994b, 1995). Therefore, the intersection of the AP-1 family proteins with the even larger number of potential CNC/small Maf interactions places these heteromeric transcription factors at the crux of a complicated, yet potentially exquisitely sensitive, regulatory network. One can envision how each of these proteins might contribute to a very sensitive ''on/off'' transcriptional switch, which could be finely titrated based simply on their relative activities inside cells at specific times during development (Engel 1994; Motohashi et al. 1997).

[3]These authors contributed equally to this work.
[4]Corresponding author.
E-MAIL d-engel@nwu.edu; FAX (847) 467-2152.

Gene targeting has revealed distinct roles for several CNC family members in mammalian gene regulation. *nrf1*-null mutants display a nonautonomous defect in mesoderm formation and fail to develop beyond embryonic day (E) 7.5 (Farmer et al. 1997). *nrf2*-null mutants, on the other hand, are viable (Chan et al. 1996; Itoh et al. 1997) but impaired in the xenobiotic inductive response of phase II drug detoxifying enzyme genes (Itoh et al. 1997). Most germane to the present study, *p45* homozygous mutant mice display profound thrombocytopenia as a result of impaired megakaryocyte differentiation, leading to postnatal death (Shivdasani et al. 1995).

Recently, the mouse *mafK* gene was disrupted by gene targeting. In contrast to *p45* and *nrf1*-null mutants, however, the *mafK* mutant mice were viable, fertile, and apparently normal and healthy (Kotkow and Orkin 1996). Because the small Maf proteins can functionally substitute for one another in vitro in the NF–E2 DNA-binding complex (Igarashi et al. 1994), it was suggested that another small Maf protein might provide a complementing activity that rescues *mafK* homozygous mutant animals. This result was somewhat disquieting, however, as MafK is not ubiquitous, but is restricted within well defined cell lineages (Motohashi et al. 1996), as are the two other small Maf proteins (J. Akasaka, in prep.). Therefore, the observation that the *mafK* germ-line mutation led to no phenotype raised the spectre that the small Maf proteins might not be required for CNC family interactions in vivo, and that the genuine partner molecule(s) required for CNC activation was yet to be defined.

To address this question, we explored the functional roles of MafG and MafK in the mouse by replacing the entire coding regions of both the *mafG* and *mafK* genes with the *lacZ* gene. No defects were observed in $mafK^{-/-}$ mice, in accord with a previous report (Kotkow and Orkin 1996). In contrast, although $mafG^{-/-}$ animals were also viable and fertile, they exhibited abnormal megakaryocyte proliferation with accompanying thrombocytopenia, as well as behavioral defects. Furthermore, the *mafG* and *mafK* genes display almost perfectly complementary expression patterns in early embryos, and the patterns of both genes become more complicated from E8.5 onward.

These results show that although the small Maf proteins can compensate for some embryonic functions when they are expressed in the same tissue, other roles of the small Maf factors are complementary and therefore cannot be fully compensated. This is most readily apparent during megakaryopoiesis and neurogenesis, where $mafG^{-/-}$ animals display physiological defects from the loss-of-function mutation, thereby demonstrating for the first time that the small Maf proteins are physiologically required in vivo.

Results

Targeting of the mafG *and* mafK *genes*

To elucidate possible roles for the small Maf proteins in murine development, we generated loss-of-function mutations in the *mafG* and *mafK* genes by deleting their entire coding sequences (J. Akasaka, in prep.; Motohashi et al. 1996). Targeting vectors were designed to replace the coding exons with selectable markers; in the case of *mafG*, loxP sites surrounded the MC1neo/MC1HSVtk cassette (Fig. 1a), whereas for *mafK*, loxP sites were placed around a phosphoglycerate kinase (PGK)–neo cassette (Fig. 1e). Immediately 5′ to these markers, and replacing the endogenous translation initiation sites present in each of the *mafG* or *mafK* second exons, the *lacZ* gene was inserted, thereby allowing the small *maf* genes to be individually monitored by X-gal staining. Diphtheria toxin and thymidine kinase were used as negative selection markers in the *mafG* and *mafK* targeting cassettes, respectively (Fig. 1a,e).

R1 embryonic stem (ES) cells (Nagy et al. 1993) were electroporated with the linearized targeting constructs, and for *mafG* targeting 19 of 456 colonies were identified as homologous recombinants by PCR (Fig. 1b); eight of these positive clones were confirmed by Southern blotting (Fig. 1c). In the case of *mafK*, five of 68 colonies were shown to be properly integrated by Southern blotting (Fig. 1f). All of the ES clones were confirmed by additional restriction enzyme digests and Southern blotting (data not shown). The selected clones were then aggregated with eight-cell diploid embryos. Two *mafG* and three *mafK* clones produced chimeras that passed the mutant alleles to first generation offspring. The chimeras were bred to both CD1 and C57BL/6J mice for subsequent studies (Fig. 1d,g).

mafK *and* mafG *homozygous null mutant animals are viable and fertile*

Heterozygous F_1 offspring were intercrossed and the resulting pups were examined and genotyped between birth and 2 weeks of age. The results of breeding experiments from the three *mafK* lines in the CD1 background showed that they displayed a normal Mendelian ratio of offspring (Table 1). *mafG* homozygous mutant mice were born at a lower than expected ratio. This result was not statistically significant ($P > 0.1$) in the C57BL/6J background, but was in the CD1 background ($P < 0.01$; Table 1). RNase protection experiments on samples taken from multiple tissues showed that both targeting events resulted in null mutations in the respective genes (H. Motohashi, unpubl.).

Impaired thrombopoiesis in mafG *mutant mice*

Because NF-E2 has been demonstrated to be a key regulatory molecule in thrombopoiesis (Shivdasani et al. 1995), and all previous literature suggested that the required partner for p45 was a small Maf molecule, we first analyzed the peripheral blood of *mafG* and *mafK* homozygous mutant animals. The platelet count was dramatically diminished in *mafG* mutant mice, whereas all other blood cell lineages were unaffected by the mutation (Table 2; data not shown). Furthermore, histological analysis revealed a threefold increase in the number of

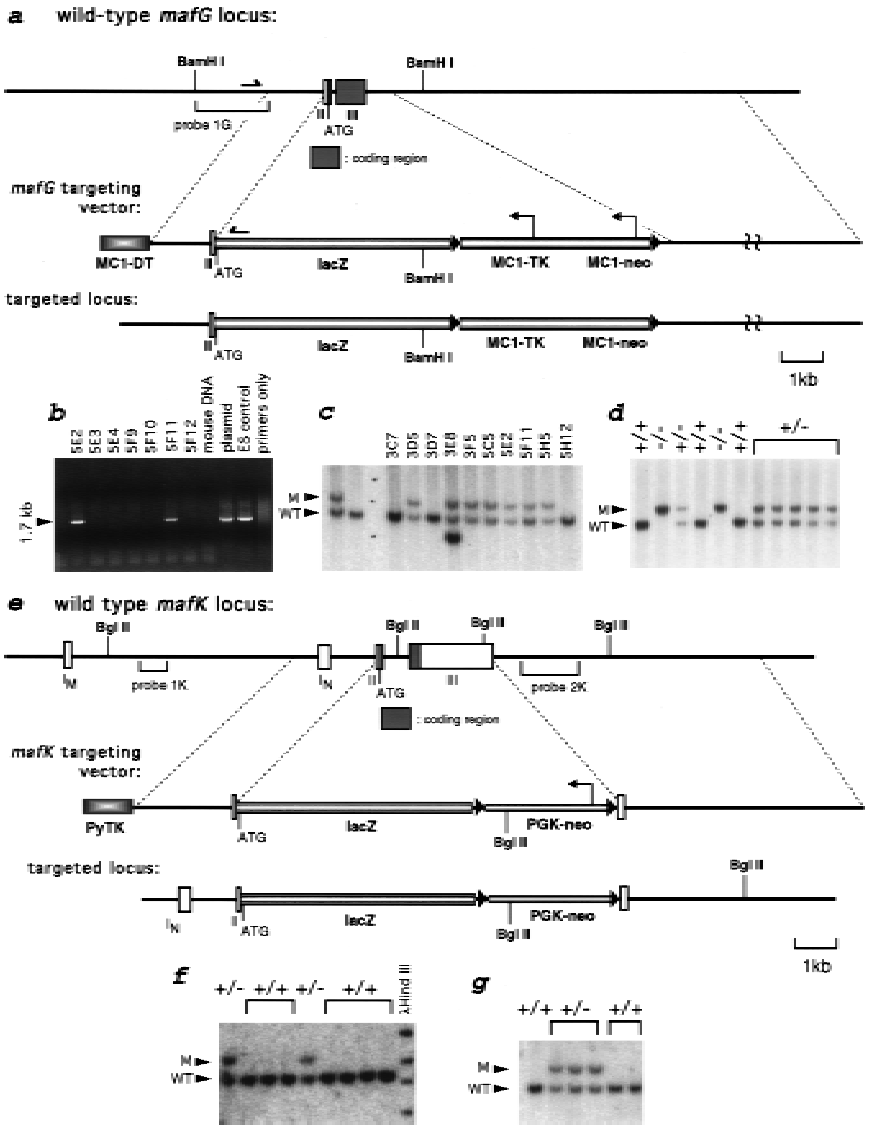

Figure 1. Targeted disruption of the *mafG* and *mafK* genes. (*a*) Structure of the *mafG* genomic locus, targeting vector, and targeted locus. (*b*) PCR screening of R1 ES cell clones using the primers whose positions are indicated by single headed arrows in *a*. (*c*) Southern blot confirmation of PCR positive and negative clones, using probe 1G, a 1.6-kb *Bam*HI–*Sac*I fragment. Clone 3E8 shows an additional band that was not seen after further expansion. (*d*) Southern blot of tail DNAs from litters of $mafG^{+/-}$ intercrosses, using probe 1G. (*e*) Structure of the *mafK* genomic locus, targeting vector, and targeted locus. (*f*) Southern blot screening of R1 ES cell clones, using probe 1K, a 6.6-kb *Xba*I fragment. (*g*) Southern blot of tail DNAs from litters of $mafK^{+/-}$ backcrosses, using probe 2K, a 1.3-kb *Sac*I–*Xba*I fragment. (M) Mutant allele; (WT) wild-type allele.

megakaryocytes in both the bone marrow and in spleen sections of $mafG^{-/-}$ animals in comparison with heterozygous littermates (Fig. 2a,b; Table 2). In addition, $mafG^{-/-}$ megakaryocytes displayed both anti-glycoprotein IIb immunoreactivity and acetylcholinesterase activity (Jackson 1973; Beckstead et al. 1986; Fig. 2c,d), indicating a late differentiation block in megakaryocyte maturation, as is also the case for *p45* mutant mice. In contrast, $mafK^{+/-}$ and $mafK^{-/-}$ mice exhibited normal hematopoietic parameters (Table 2; data not shown), consistent with earlier results (Kotkow and Orkin 1996). Therefore, MafG is required for terminal differentiation

Table 1. *Genotype ratios from heterozygous small* maf *mutant intercrosses*

Mutant	+/+	+/−	−/−	Total	χ^2 test (*P*)
mafG					
C57BL/6J	29 (29%)	53 (52%)	19 (19%)	101 (100%)	>0.1
CD1	39 (36%)	53 (49%)	16 (15%)	108 (100%)	<0.01
mafK					
CD1(A3)	12 (15%)	40 (51%)	27 (34%)	79 (100%)	>0.05
CD1(B2)	16 (33%)	24 (50%)	8 (17%)	48 (100%)	>0.1
CD1(D1)	30 (26%)	62 (54%)	23 (20%)	115 (100%)	>0.1

The *mafG* data are from one chimera crossed into either the C57BL/6J or CD1 genetic background. The *mafK* matings are for three different ES clones (in parentheses), all bred into the CD1 background.

Table 2. *Hematopoietic analysis of the small* maf *mutants*

Genotype	Platelet count ($\times 10^3$/μl)	Megakaryocytes (% nucleated cells)[a]
$mafG^{+/-}$	1213.7 ± 46.4	0.050 ± 0.017
$mafG^{-/-}$	541.7 ± 48.4	0.147 ± 0.038
$mafK^{+/-}$	1267.7 ± 17.2	N.D.
$mafK^{-/-}$	1095.0 ± 58.1	N.D.

Whole blood and bone marrow were harvested from *mafG* and *mafK* mutant littermates, and the platelet count and megakaryocyte percentage were determined on three different animals of each genotype (see Materials and Methods).
[a](N.D.) Not determined.

during thrombopoiesis, demonstrating for the first time a functional requirement for a small Maf protein.

Behavioral analysis reveals additional MafG functions in the nervous system

Further observations indicated that the $mafG^{-/-}$ pups might display deficits in addition to the one identified in hematopoiesis. These unexpected deficiencies appeared to be of neuronal origin, and were more obvious in the C57BL/6J than in the CD1 background, and therefore we report observations only in C57BL/6J mice.

The presumptive neurological defect was first noted when newly weaned mice were held inverted by the tail during cage changes, where homozygous mutant pups could be easily and uniformly identified by their response to handling. Instead of employing a typically smooth sideways motion to reach upward, as in their wild-type or heterozygous littermates, $mafG^{-/-}$ pups convulsively attempted to throw themselves into an upright position (data not shown). This behavior became less obvious as the mice aged (5–6 months), but was replaced by a new behavior, clasping their hindlegs together when inverted, another uncharacteristic response which is not observed in heterozygous littermates or wild type animals (Fig. 3a).

To quantify these behavioral abnormalities, we initially tested the animals in some simple behavioral tasks. $mafG^{-/-}$ adults were permitted to grab a thin wire with their forepaws, and were then left to hang, and their responses examined. Wild-type or heterozygous mutant animals immediately grabbed the wire with their hindpaws and were able to hold themselves or balance on top of the wire for an average of 51 sec. The majority of homozygous *mafG* mutants, on the other hand, were unable to grasp the wire with their hindlimbs—they hung briefly before dropping to the surface below (Table 3). A second test, that would not so obviously require well developed musculature, was performed by placing the mice on a 10-ml glass pipette. The results were the same as for the wire hang task—nearly all $mafG^{-/-}$ animals were unable to support themselves for longer than 15 sec, whereas littermates could maintain this balanced position for 1 min (the test time limit; Table 3).

To characterize the *mafG* mutant animals more extensively, we subjected them to a battery of additional neurological tests (Crawley and Paylor 1997) and to open field testing. Heterozygous and homozygous mutants were indistinguishable in appearance (except in size, below) or gross neurological behavior in an empty cage; furthermore, in several additional tests (swimming, rearing, rolling, righting), $mafG^{+/-}$ and $mafG^{-/-}$ animals responded similarly. In the open field test, we found no statistically significant differences in time spent in the center or periphery of the field, number of squares traversed, number of rearings, freezing time, or number of fecal boli ($n = 4$ $mafG^{+/-}$, $n = 8$ $mafG^{-/-}$; data not shown). Therefore, the effect(s) of the *mafG* mutation on the nervous system, although very restricted, appears to be fully penetrant.

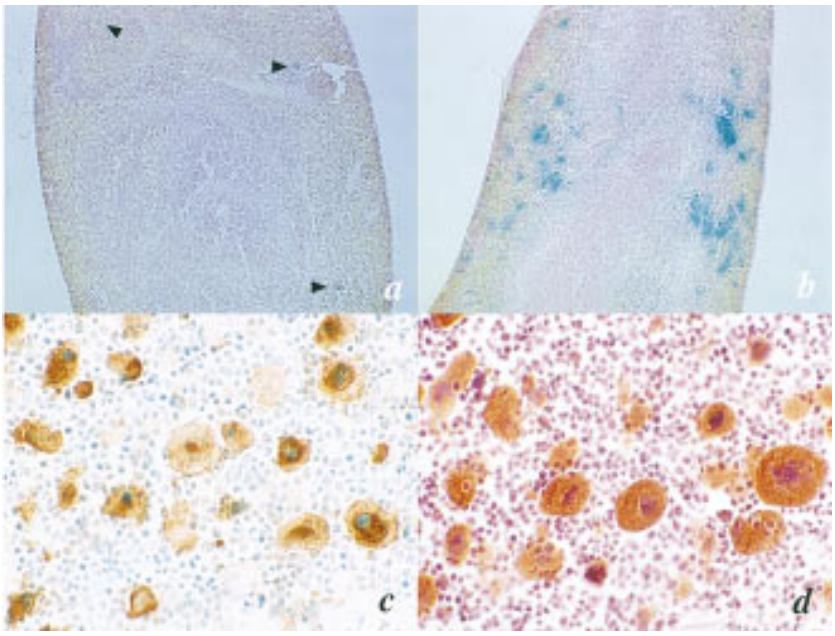

Figure 2. Stimulation of megakaryopoiesis in *mafG* mutant mice. (*a*) A transverse section through a $mafG^{+/-}$ adult spleen shows few β-gal staining megakaryocytes (indicated by arrowheads). (*b*) A similar section through the spleen of a $mafG^{-/-}$ littermate shows expansion of the megakaryocyte population. In addition, these show a dosage dependent increase in staining, attributable to the presence of one additional expressed copy of *lacZ*. $mafG^{-/-}$ megakaryocytes from adult bone marrow are positive for anti-glycoprotein IIb antibody reactivity (*c*) and for acetylcholinesterase activity (*d*) (Jackson 1973; Beckstead et al. 1986).

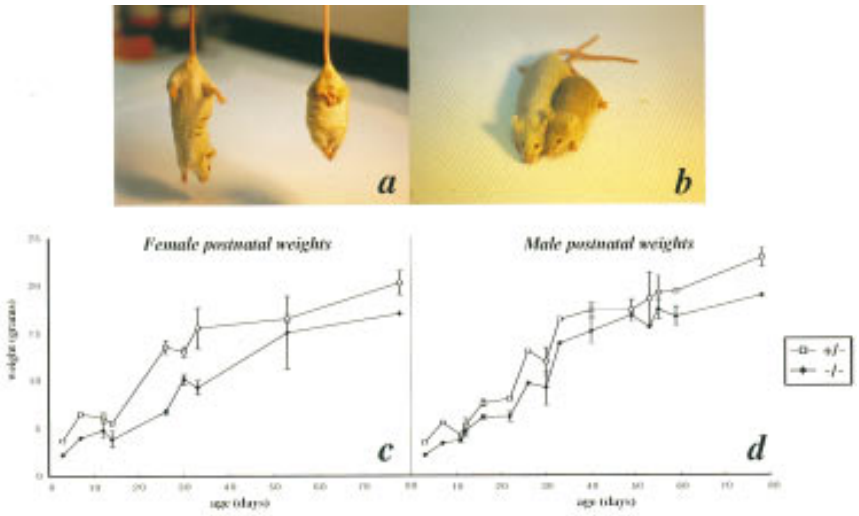

Figure 3. Behavioral and weight deficits in *mafG* mutant animals. (*a*) Six-month-old $mafG^{+/-}$ (*left*) and $mafG^{-/-}$ (*right*) male littermates display wild-type and abnormal behaviors, respectively. Homozygous mutant animals spontaneously clench their hindlegs together when suspended in an inverted position. (*b*) A photograph of the mice in *a* shows that the $mafG^{-/-}$ mutant (*right*) is smaller than its heterozygous littermate (*left*). (*c*,*d*) Developmental profile of *mafG* postnatal weights in B6/129 background animals. Heterozygous (□) and homozygous (♦) mutant littermates were weighed and averaged from the first week after birth up to 11 weeks of age.

mafG *homozygous mutants are subject to postnatal wasting*

The small *maf* homozygous mutant animals survived beyond weaning with no apparent difficulty. Some $mafG^{-/-}$ animals, however, were obviously smaller than their littermates (Fig. 3b). This was quantified by weighing pups at different ages; *mafG* mutant pups showed a significant disparity from their littermates postnatally through adulthood. This was found in both the C57BL/6J (Fig. 3c,d) and CD1 (not shown) backgrounds. In almost all litters examined, homozygous mutant females weighed less than their littermates (Fig. 3c), but this phenotype was less penetrant for males (Fig. 3d). We averaged the weights of the wild-type and heterozygous animals (these two classes did not show any significant disparities) from individual litters, and then calculated the normalized percentage of each individual relative to its litter average for all time points examined. These values showed that $mafG^{-/-}$ females and males had respective mean weights of 71.2% and 82.3% of the $mafG^{+/+}$ and $mafG^{+/-}$ animals. Once again, *mafK* homozygous mutants exhibited no similar discrepancy (data not shown).

Complementary expression of the mafK *and* mafG *genes during murine embryogenesis*

To elucidate further the molecular mechanisms that might underlie the *mafG* gene null mutant-specific phenotypes, we characterized the *mafG* and *mafK* expression patterns using the inserted *lacZ* genes as reporters to detect β-galactosidase (β-gal) activity. The rationale for this analysis was that if the *mafG*-specific phenotypes were attributable to a lack of compensation by other small Maf proteins, we might be able to identify nonoverlapping sites of expression of both the *mafG* and *mafK* genes through such an analysis. Matings were therefore conducted between heterozygous animals of a mixed 129/CD1 background, and the litters were examined at E6.5, E7.5, E8.5, E9.5, E10.5, E12.5, and E14.5. At stages after E9.5, embryos were genotyped by PCR.

Although differences were not observed either in embryonic development or in staining patterns between heterozygous versus homozygous mutant embryos, the homozygous mutants showed uniformly more intense staining (data not shown). In embryos that were not genotyped (before E9.5), three staining classes were observed—lesser staining (presumed to be heterozygous), more intensely staining (presumptive homozygous mutant), and no visible staining (classified as wild type).

At E6.5, to our surprise, *mafG* and *mafK* exhibited almost perfect mutually exclusive staining patterns (Fig. 4a,b). A comparison of the $mafG^{-/-}$ and $mafK^{-/-}$ whole-mount stained embryos displayed an obvious and striking contrast—*mafG* and *mafK* expression clearly demarcated the epiblast/extraembryonic boundary. *mafG* was clearly expressed in the embryonic ectoderm and mesoderm, with very weak staining in extraembryonic tissues. In contrast, *mafK* mutant embryos intensely stained the ectoplacental cone and extraembryonic endoderm. Although the two genes shared a spotted staining pattern across the entire embryo, which was not observed in wild-type embryos (data not shown), it was unclear from this analysis alone whether or not the two spotted patterns overlapped. At E7.5, the expression pat-

Table 3. mafG *mutant behavioral phenotypes*

Genotype	Wire hang time (sec)	Balancing time (sec)
+/−	51 ± 15	47 ± 21
−/−	17 ± 21	15 ± 21
t-test	$P = 4.4 \times 10^{-7}$	$P = 1.6 \times 10^{-4}$

mafG homozygous mutants and heterozygous littermates were subjected to the wire hang and balancing tasks, as described (Materials and Methods).

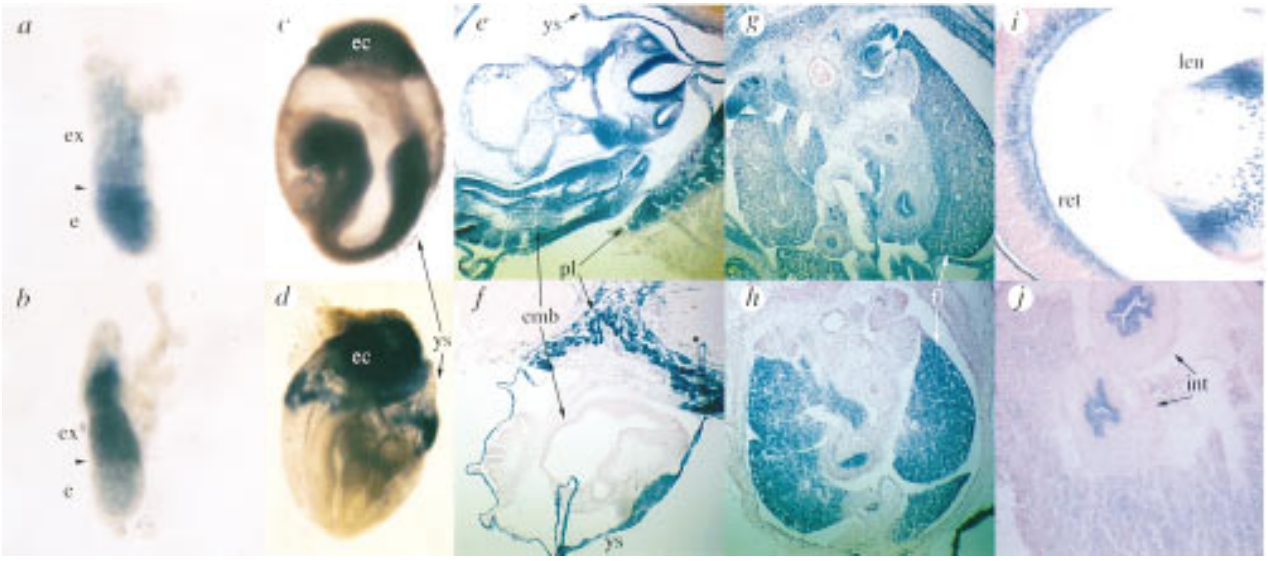

Figure 4. Embryonic expression patterns of *mafG* and *mafK*. *mafG*$^{-/-}$ (*a*,*c*,*e*,*g*,*i*) and *mafK*$^{-/-}$ (*b*,*d*,*f*,*h*,*j*) embryos were dissected, fixed, and stained for β-gal activity as described in Materials and methods. (*a*,*b*) Whole-mounts of E6.5 embryos show that *mafG* expression is detected strongly in embryonic tissues, whereas *mafK* is predominantly extraembryonic. Both genes are expressed in a diffuse pattern in the complementary region of the embryos. (*c*,*d*) E8.5 embryos show that *mafG* and *mafK* continue to be embryonic and extraembryonic, respectively, with expansion of both into the ectoplacental cone, and *mafK* initiating expression in the yolk sac endoderm. (*e*,*f*) Transverse sections through E9.5 embryos indicate expression of *mafG* in the embryo, placenta, and yolk sac, with *mafK* limited to the placenta and yolk sac endoderm. (*g*,*h*) At E12.5, transverse sections of *mafG* and *mafK* stained embryos exhibit strong expression in the hematopoietic compartment of the fetal liver. (*i*) A transverse section of an E14.5 embryo shows strong *mafG* staining in the developing lens and retina. (*j*) At E14.5, the strongest site of *mafK* expression is seen specifically in the intestinal epithelium. (Arrowheads in *a* and *b*) Embryonic/extraembryonic boundary; (e) embryonic pole of the egg cylinder; (ex) extraembryonic pole of the egg cylinder; (ec) ectoplacental cone; (ys) yolk sac; (emb) embryo; (pl) placenta; (fl) fetal liver; (ret) retina; (len) lens epithelium; (int) intestine.

terns for both genes were essentially unchanged, with *mafG* expressed throughout most of the embryo and *mafK* expressed primarily in developing extraembryonic endoderm (data not shown).

At E8.5, *mafG* expression was still strong throughout the entire embryo, with especially intense staining in the neural tube. At this stage, the *mafG* pattern began to intensify in the ectoplacental cone but only weakly stained the extraembryonic tissues (Fig. 4c). This same pattern persisted into E9.5 (Fig. 4e), when weak staining in the yolk sac blood islands first became detectable. At E8.5, *mafK* staining was also intense in the ectoplacental cone and in the yolk sac visceral endoderm (Fig. 4d). By E9.0 the entire yolk sac endoderm displayed very intense *mafK* staining. Weak neural tube expression of *mafK* became apparent, and this continued into E9.5 along with the yolk sac and ectoplacental cone staining (Fig. 4f). *mafG* continued to be expressed throughout almost the entire embryo at E9.5, E12.5, and E14.5 (Fig. 4g; data not shown). Some additional sites of particularly intense *mafG* expression were in the epithelium of the intestine, skeletal muscle, lens and retina, brain, and both cranial nerve and dorsal root ganglion cells (Fig. 4i; data not shown). In contrast to the quite broad embryonic expression of *mafG*, during this same period *mafK* was restricted to intense staining in the placenta, hematopoietic cells of the fetal liver (Fig. 4h), yolk sac endoderm, epithelium of the intestine (Fig. 4j), and the heart (data not shown).

After birth, both *mafG* and *mafK* were strongly expressed in the epidermis, hair follicles, epithelium of the digestive and respiratory tracts, and kidney tubules (data not shown). Many of these are proliferating tissues, implying that the small Maf proteins may have particularly important roles in cell growth or division. In adult mice, *mafG* and *mafK* displayed expression in both overlapping as well as individually distinct tissues. In some, such as tubules of the kidney, both *mafG* and *mafK* were strongly expressed, but in other tissues, one was far more predominant (see below).

Differential expression of mafG *and* mafK *suggests mechanisms for* mafG$^{-/-}$*-specific phenotypes*

As *mafG* mutant mice showed a specific thrombopoietic phenotype, we sought to investigate this defect further by analyzing β-gal activity in megakaryocytes synthesized in either *mafG* or *mafK* mutant animals. During embryonic development, at E12.5, we found that *mafG* (Fig. 5a) and *mafK* (Fig 5b) were both expressed strongly in differentiating megakaryocytes of the fetal liver, as well as in newborn pups (data not shown). Adult mice (>2 months), however, showed differential expression. Whereas *mafG* was strongly expressed in adult mega-

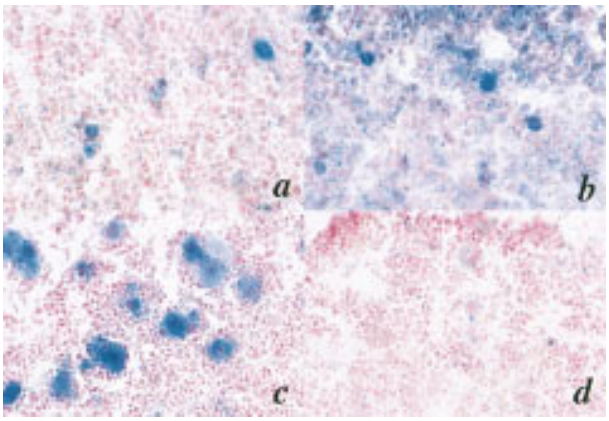

Figure 5. Small *maf* expression in megakaryocytes. E12.5 fetal liver (*a*,*b*) and adult bone marrow (*c*,*d*) were isolated, fixed, and stained for *lacZ* expression as described (Materials and methods). (*a*) $mafG^{-/-}$ and $mafK^{-/-}$ (*b*) E12.5 embryos display similar intensities of β-gal activity in fetal liver megakaryocytes. (c) *mafG* exhibits intense expression in adult mutant megakaryocytes, whereas *mafK* expression is much weaker (*d*).

karyocytes (Fig. 5c), *mafK* was only weakly expressed there (Fig. 5d). These data indicate that *mafG* is the predominant small Maf protein functioning in thrombopoiesis during the adult stage.

We sought to understand the underlying mechanism responsible for the behavioral phenotype. Motor behavior is a product of first sensing body position, followed by the ability to respond and modulate this position. The former function is performed by the vestibular system (saccule and utricle) and the semi-circular canals of the inner ear, whereas the latter is carried out by the cerebellum. We postulated that either (or possibly both) of these tissues might represent sites of prominent *mafG* expression. If so, and if *mafK* were not expressed there, then a tissue defect at either site would become an excellent candidate as the basis of the observed neurological $mafG^{-/-}$ mutant phenotypes.

Because the area of the inner ear is firmly embedded in bone in adults and decalcification would destroy any β-gal activity there, we examined the developing vestibular system in newborn animals. These experiments showed that vestibular ganglia and sensory cells of the saccule specifically expressed *mafG*, but not *mafK* (Fig. 6a; data not shown). In addition, *mafG* was expressed strongly in the cerebellum (Fig. 6b), whereas *mafK* was not (Fig. 6c). Therefore, it is possible that deficiencies in either or both of these neurological systems may underlie the observed behavioral deficits.

Discussion

We have carried out a genetic loss-of-function analysis for two of the three small Maf proteins, and also have analyzed the expression profiles of these two small *maf* genes using a β-gal reporter inserted into each locus. Whereas MafG and MafK display overlap in expression at several sites and during several periods where the two might provide compensatory activity, there are also many sites and times during development where expression of the two factors is not overlapping, and therefore they certainly cannot compensate for one anothers' activities there. We show here that, individually, MafG and MafK are both dispensable for mouse viability and fertility. In each homozygous null mutant animal, the remaining two small Maf proteins can presumably compensate for the loss of any one. These data also show, however, that there are at least two functions for MafG, in megakaryocyte differentiation and neural development, which are not fully compensated by residual MafK and/or MafF expression. These results therefore provide the first direct proof that the small Maf proteins are required for specific physiological functions during development.

One of the three major $mafG^{-/-}$-specific phenotypes is thrombocytopenia. This phenotype is especially intriguing in that, in mice bearing a *p45* gene disruption, ~90% of the homozygous mutants die of severe hemorrhage, secondary to nearly complete thrombocytopenia caused by a late block in megakaryocyte maturation (Shivdasani et al. 1995). Similarly, MafG-deficient mice are impaired in producing platelets, but do not show a propensity to hemorrhage. The most likely interpretation of these data

Figure 6. Neuronal *mafG* and *mafK* expression. Newborn and adult mice were sacrificed, their organs dissected, fixed, and stained for β-gal activity as described (Materials and methods). (*a*) The inner ear of newborn pups shows *mafG* expression in the vestibulocochlear ganglion (arrowhead) and saccule sensory epithelium (arrow). (*b*) Adult cerebellar Purkinje and granular cells exhibit high levels of *mafG*, but no detectable *mafK* (*c*). (co) Cochlea.

is that MafG is the predominant partner molecule of p45 during megakaryopoiesis. Presumably a low level of residual MafK and/or MafF expression in megakaryocytes partially sustains thrombopoiesis, and therefore the phenotype of MafG deficiency is less severe than the loss of p45 (i.e., the *mafG* loss-of-function mutation is a hypomorphic phenocopy of the homozygous *p45* mutation). In addition to the platelet deficiency, the number of megakaryocytes increases in the bone marrow and spleens of *mafG* mutant animals. This may be attributable to a combination of maturation arrest at the final stage of megakaryocytic differentiation caused by a lack of active NF-E2 (p45:MafG heterodimer) activity, as well as to a compensatory homeostatic increase in megakaryocyte proliferation induced in response to the decreased platelet number.

The second phenotype displayed by $mafG^{-/-}$ mice is age-dependent behavioral abnormalities. In two simple behavioral tasks, *mafG* homozygous mutant adults were quantifiably different than their wild-type and heterozygous littermates, confirming suspicions of a vestibular, neurological, or muscle defect, whereas the results of the balancing task imply that the defect is probably not muscular in origin. Furthermore, there are quite distinct differences in expression of the two proteins in the CNS, where MafG/*lacZ* is far more strongly expressed, implying that MafG is also much more abundant (in the forebrain, midbrain, cerebellum, retinal ganglion cell layer, and the sensory epithelium of the internal ear) than is MafK. We conclude that loss of MafG results in a neurological defect, probably within the cerebellum or the inner ear, although the detailed physiological abnormalities specifically responsible for the observed behavioral phenotypes are yet to be determined.

Tracing the ''knock-in'' reporter gene activity during embryogenesis defined a strikingly distinct pattern of expression of the *mafG* and *mafK* genes as early as E6.5. At this point in development, the expression of these two small Mafs essentially defines the junction between extraembryonic and embryonic tissues. On the other hand, especially after birth, the expression patterns of MafG and MafK expand and become complex, encompassing many different tissues and organs. In particular, we note that many sites of expression are proliferating tissues, such as epidermis, hair follicles, digestive and respiratory tract epithelia, and bone marrow, implying that the small Mafs may also have a role in cell growth or division.

The embryonic expression patterns and apparent lack of embryonic developmental phenotypes for *mafG*- and *mafK*-mutant mice beg the question: Do these small Mafs compensate for one another during development? There are two possible ways in which such compensation could occur. When one of the small Maf genes is mutated, the overlapping expression of another might contribute to the required activity. Alternatively, ablation of one gene could induce the expression of either one or both of the two remaining small *maf* genes in that tissue. These possibilities should be considered for several key times and sites of small *maf* expression, such as the yolk sac from E9.5–10.5, or in the fetal liver at E12.5, where both of these small Maf proteins are expressed at high levels. To determine if these represent important sites and/or times during development when the small *maf* genes must compensate for one another, it will be necessary to generate and examine compound $mafG^{-/-}$::$mafK^{-/-}$ mutant animals. If these genes are compensatory in the yolk sac or fetal liver, one should observe lethality in the compound mutants before, or during, this crucial period (E9.5–E12.5) when the embryo switches from primitive to definitive hematopoiesis (Copp 1995). Strong expression of *mafG* and *mafK* is also detected in the ectoplacental cone beginning at E8.5 and continues in the placenta through E14.5, so the possibility also exists that uncompensated compound mutants might die during this time frame. In the latter scenario, the small Mafs could be critical for forming a normal placenta to ensure the transition from diffusion-based to placental nutrition (Copp 1995). These intercross mating experiments, as well as detailed expression analysis of the small Mafs in the mutant mice, are ongoing.

Materials and methods

Construction and preparation of targeting vectors

The vector ploxPneo1 (the gift of A. Nagy, Mount Sinai Hospital, Toronto, Ontario, Canada) was used to construct the *mafK* targeting vector. It contains a mutant neomycin resistance gene derived from pPNT (Tybulewicz et al. 1991) flanked by loxP sites and driven by the mouse PGK promoter. To construct ploxPneo–HA–SS–β-gal, the *Sma*I–*Not*I and *Not*I–*Sal*I fragments (coding region and poly(A) signal of *Escherichia coli* β-gal, respectively) were excised from pSVβ (Clontech) and cloned into the *Eco*RV and *Hin*dIII—*Sal*I sites of pBluescript SK+ (pBS), respectively (pβ-gal). Next, a 1.8-kb *Sma*I–*Sma*I fragment containing 5′ genomic sequence and exon IN was inserted into the pBS *Eco*RI site of pβ-gal. Finally, an *Xho*I–*Hin*dIII fragment that contains the herpes simplex thymidine kinase gene flanked by polyoma virus enhancers (PyTK; Mansour et al. 1988) was inserted into the *Sma*I site in the pBS polylinker. Ligation of blunted *Xho*I and *Sma*I sites regenerated the *Xho*I site, and a clone with this *Xho*I site opposite β-gal was selected, and designated pTK–SS–β-gal.

A 6.6-kb *Hin*dIII–*Asc*I genomic fragment of *mafK* containing the 3′ end of the third exon and 3′ flanking sequences was cloned into the *Sma*I site of ploxPneo1 (ploxPneo–HA). Next, the *Xho*I fragment from pTK–SS–β-gal, consisting of PyTK, *mafK* sequences, and β-gal, was inserted into the *Xho*I site of ploxPneo–HA, thus completing ploxPneo–HA–SS–β-gal (ploxPneo–β-gal). This vector deleted the second and third (both coding) exons, and left β-gal under control of the *mafK* locus.

The *mafG* targeting vector was constructed using the plasmid pNATA (the generous gift of Y. Nabeshima, National Institute of Neuroscience, Tokyo, Japan). This plasmid contains the neomycin resistance and thymidine kinase (*neo/TK*) genes, each driven by individual MC1 promoters (Mansour et al. 1988) and flanked by loxP sites. The gene for diphtheria toxin subunit A (DT), also transcriptionally directed by the MC1 promoter, was added for negative selection. A 1.4-kb *Sac*I–*Sma*I genomic fragment containing the 5′ end of the second exon was inserted into the *Eco*RI site of pβ-gal, creating pScSm–β-gal. An 8.0-kb *Eco*RV–*Sal*I genomic fragment downstream from the presumed third exon was inserted into the *Hpa*I site of pNATA (pNATA–EVSI).

Finally, the *Not*I–*Sal*I fragment from pScSm–β-gal was cloned into the *Sal*I site of pNATA–EVSI, creating the targeting Vector pNATA–DT–EVSI. This construct deleted the second and third exons, leaving *lacZ* under control of the *mafG* locus.

Gene targeting in ES cells

R1 ES cells (Nagy et al. 1993) were cultured on mitomycin C-treated primary mouse embryonic fibroblast feeders (prepared according to Hogan et al. 1994) on gelatinized tissue culture plates essentially as described (Wurst and Joyner 1993). The medium consisted of high glucose Dulbecco's Modified Eagle Medium (DMEM) and 15% fetal bovine serum (FBS, HyClone), supplemented with non-essential amino acids, glutamine, sodium pyruvate, β-mercaptoethanol, penicillin/streptomycin, and 1000 units/ml of leukemia inhibitory factor (ESGRO, GIBCO-BRL).

ploxPneo–β-gal and pNATA–DT–EVSI were linearized with *Not*I, extracted with phenol:chloroform, precipitated, and resuspended in TE buffer. The R1 cells were trypsinized and resuspended in either PBS or ES medium, and from 5.6 to 10×10^6 cells were electroporated with 25 μg of linearized targeting vector at 240 V, 500 μF, and placed on ice for 20 min. Each cuvette was subsequently plated on a 100-mm plate of feeder cells derived from a mouse containing the gene for neomycin resistance (Genome Systems or The Jackson Laboratory). The cells were cultured for 24–48 hr before G418 (GIBCO-BRL) and Gancyclovir (Syntex) were added at concentrations of 210 μg/ml (active component) and 2 μM, respectively. Medium was changed daily, and selection was maintained for 8 days, by which time colonies were visible to the naked eye.

Individual colonies were picked under 10–40 × magnification, grown on feeders in 96-well plates, and replica-plated, using one plate for DNA and the other as a frozen stock, as described (Ramirez-Solis et al. 1992). In the case of *mafK* targeting, 68 colonies were screened by Southern blotting using a 5′ external probe (a 0.6-kb *Xba*I fragment 2.0-kb 3′ to exon IM), which identified 5 colonies with a 10.0-kb mutant *Bgl*II fragment in addition to the 6.9-kb endogenous fragment. For *mafG*, PCR screening was performed using a 5′ primer just upstream of the short arm *Sac*I site, and a 3′ primer in the 5′ region of the *lacZ* gene. Twenty-one clones were identified, yielding a targeting frequency of 1 in 22. Eight were confirmed by Southerns to be properly targeted clones by the presence of a polymorphic 6.4-kb *Bam*HI fragment, in addition to the wild-type 5.3-kb fragment.

Generation of mutant mice

Chimeric mice were derived as described (Nagy and Rossant 1993) except that single eight-cell diploid embryos from CD1 egg donors (Charles River) were used for each aggregation. The aggregates were cultured overnight, and 8–12 blastocysts were transferred to each uterine horn of pseudopregnant CD1 females. Chimeras of greater than 50% ES cell contribution (estimated by coat color) were mated to CD1 females. Three *mafK* and two *mafG* targeted ES clones passed the mutation to F_1 offspring. Subsequently, the transmitting chimeras were mated to C57BL/6J mice to transfer the mutant allele to this background.

Genotyping of progeny was done by Southern blot and PCR analysis of tail DNA (Hogan et al. 1994). Briefly, the tips of mouse pup tails were digested overnight in lysis buffer [100 mM NaCl, 1.0% SDS, 50 mM Tris (pH 8.0), 100 mM EDTA (pH 8.0), 0.35 mg/ml fresh proteinase K] at 55°C, phenol/chloroform extracted, and precipitated. For PCR analysis, a common primer 5′ to exon 2 and two alternative 3′ primers were designed to detect the three classes of progeny in a single PCR reaction. The 3′ primer that detected the wild-type allele was in the second intron, whereas the 3′ mutant allele primer corresponded to the 5′ region of the *lacZ* gene.

Staining for lacZ *gene (β-gal) activity*

The inserted *lacZ* gene was used to follow the small *maf* expression pattern by staining with X-gal (5-bromo-4-chloro–3-indolyl-β-D–galactoside). 129/CD1 hybrid mice were used for these experiments. Noon on the day that a copulation plug was detected was considered day 0.5 of pregnancy. Pregnant females were sacrificed on the desired dates, and embryos were dissected and then immersed in fixative (1% formaldehyde, 0.2% glutaraldehyde, 0.02% NP-40 in PBS) at 4°C for 2 hr. After washing with PBS, the embryos were soaked in 20% sucrose overnight, and then embedded in OCT compound (Tissue-Tek, Sakura) and sectioned in a cryostat at −20°C. Subsequently, the embryos were stained with X-gal solution [0.1 M sodium phosphate at pH 7.3, 2 mM $MgCl_2$, 5 mM $K_3Fe(CN)_6$, 5 mM $K_4Fe(CN)_6$, 0.01% sodium deoxycholate, 0.02% NP-40, 20 mM Tris-HCl, 1 mg/ml of X-gal] at 37°C overnight, and counterstained with nuclear fast red. Alternatively, embryos younger than E9.5 were usually stained at 30°C after fixation, and then processed as described above.

Assaying for glycoprotein IIb immunoreactivity and acetylcholinesterase activity

Femurs from 2- to 4-month-old $mafG^{-/-}$ animals were dissected and opened before fixation in 4% paraformaldehyde for 2 hr at 4°C, followed by overnight immersion in 20% sucrose. Bone marrow was then removed and embedded in OCT compound (Tissue-Tek, Sakura) and sectioned in a cryostat at −20°C. We incubated a new rat anti-mouse glycoprotein IIb monoclonal antibody (M. Yamamoto, unpubl.) with the sectioned bone marrow, followed by incubation with horseradish peroxidase-conjugated anti-rat IgG. Diaminobenzidine was used as chromogen, labeling positive cells with a brown color, followed by counterstaining with methyl green.

Acetylcholinesterase activity was determined essentially as described (Jackson 1973). Briefly, the sectioned bone marrow was incubated for 1 hr at 37°C in a freshly prepared buffer containing 10 mg of acetylthiocholine iodide (Sigma) dissolved in 15 ml of 0.1M sodium phosphate (pH 6.0), with 1 ml of 0.1 M sodium citrate, 2 ml of 30 mM cupric sulfate, and 2 ml of 5 mM potassium ferricyanide. Positive cells became orange, and hematoxylin was used for counterstaining.

Hematological analysis

Four-month-old mice were euthanized with carbon dioxide and 0.5 ml of blood was drawn from the inferior vena cava into a syringe containing 5–10 μl of 0.5 M EDTA. The blood samples were analyzed by Anilytics, Inc. (Gaithersburg, MD).

The megakaryocyte percentage was determined by counting cells in the bone marrow. Femurs or tibias from $mafG^{+/-}$ and $mafG^{-/-}$ animals were dissected and flushed with PBS. Bone marrow cells were disaggregated by repeated flushing through a 21 gauge needle. Non-nucleated cells were removed by osmotic lysis with a hypotonic NH_4Cl solution. The remaining cell suspension was counted in a 200 μm depth hemocytometer to allow free flow of megakaryocytes. The megakaryocyte percentage was calculated as follows:

$$\text{megakaryocyte \%} = \frac{\text{megakaryocyte count}}{\text{nucleated cell count}} \times 100$$

Behavioral analysis

F_2 (129/B6) $mafG^{+/-}$ and $mafG^{-/-}$ mice were intercrossed to generate F_3 pups for behavioral testing. Animals were tested at 3–6 months of age. For the wire hang test, a wire ~2 mm in diameter was employed. Mice were allowed to grab the wire with their forepaws, and then released so their hindlimbs dangled below. Timing was initiated after the mice were released, for a maximum of 1 min. For the balancing task, the mice were placed on a 10-ml pipette with their A/P axis parallel to the pipette. Again, timing began after the mice were released, with a 1 min limit.

Weights

Mice were weighed on a balance that measured to the nearest 0.1 gram. Mice younger than 5 days old (P5) were weighed to the nearest 0.1 gram. Mice older than 5 days were weighed to the nearest 0.5 gram because of their increased activity. The entire litter was examined at every time point for reference. To control for variation between different litters, a normalized percentage (norm%) was calculated as follows, where ''normal litter mean'' is the average weight of +/+ and +/− animals from a particular litter at a particular time point.

$$\text{norm } \% = \frac{\text{individual weight}}{\text{normal litter mean}} \times 100$$

Acknowledgments

We thank Y. Tanimoto and J. Fan for outstanding technical assistance; D. Williams, J. Rossant, A. Nagy, M. Gertsenstein, and A. Cheng for advice on ES cell culture and morula aggregation; Y. Nabeshima for the pNATA plasmid; A. Nagy for ploxPneo1; M. Capecchi for PyTK; L. Solberg and F. Turek for advice on open field testing; and R. Paylor and M. McDonald for advice on behavioral analysis. We also thank J. Bungert, K. Igarashi, T. Komeno, Q. Liu, K. Tanimoto, K.-C. Lim, and R. Yu for advice and encouragement. This work was supported by a Medical Science Training Program training grant to Northwestern University (GM08152; J.A.S.) and research grants from the Ministry of Education, Science, Sports and Culture (H.M. and M.Y.), the Japanese Society for Promotion of Sciences (M.Y.), and the National Institutes of Health (HL24415 and GM28896; J.D.E.).

The publication costs of this article were defrayed in part by payment of page charges. This article must therefore be hereby marked ''advertisement'' in accordance with 18 USC section 1734 solely to indicate this fact.

References

Andrews, N.C., H. Erjument-Bromage, M.B. Davidson, P. Tempst, and S.H. Orkin. 1993a. Erythroid transcription factor NF-E2 is a haematopoietic-specific basic-leucine zipper protein. *Nature* **362:** 722–728.

Andrews, N.C., K.J. Kotkow, P.A. Ney, H. Erdjument-Bromage, P. Tempst, and S.H. Orkin. 1993b. The ubiquitous subunit of erythroid transcription factor NF-E2 is a small basic-leucine zipper protein related to the v-*maf* oncogene. *Proc. Natl. Acad. Sci.* **90:** 11488–11492.

Beckstead, J.H., P.E. Stenberg, R.P. McEver, M.A. Shuman, and D.F. Bainton. 1986. Immunohistochemical localization of membrane and alpha-granule proteins in human megakaryocytes: Application to plastic-embedded bone marrow biopsy specimens. *Blood* **67:** 285–293.

Blank, V. and N.C. Andrews. 1997. The Maf transcription factors: Regulators of differentiation. *Trends Biol. Sci.* **22:** 437–441.

Caterina, J.J., D. Donze, C.-W. Sun, D.J. Ciavatta, and T.M. Townes. 1994. Cloning and functional characterization of LCR-F1: A bZIP transcription factor that activates erythroid-specific, human globin gene expression. *Nucleic Acids Res.* **22:** 2383–2391.

Chan, J.Y., X.-L. Han, and Y.-W. Kan. 1993. Cloning of Nrfl, an NF-E2-related transcription factor, by genetic selection in yeast. *Proc. Natl. Acad. Sci.* **90:** 11371–11375.

Chan, K., R. Lu, J.C. Chan, and Y.W. Kan. 1996. NRF2, a member of the NFE2 family of transcription factors, is not essential for murine erythropoiesis, growth, and development. *Proc. Natl. Acad. Sci.* **93:** 13943–13948.

Copp, A.J. 1995. Death before birth: Clues from gene knockouts and mutations. *Trends Genet.* **11:** 87–93.

Crawley, J.N. and R. Paylor. 1997. A proposed test battery and constellations of specific behavioral paradigms to investigate the behavioral phenotypes of transgenic and knockout mice. *Hor. & Behav.* **31:** 197–211.

Engel, J.D. 1994. Meticulous AP-1 factors [Maf]. *Nature* **367:** 516–517.

Farmer, S.C., C.W. Sun, G.E. Winnier, B.L. Hogan, and T.M. Townes. 1997. The bZIP transcription factor LCR-F1 is essential for mesoderm formation in mouse development. *Genes & Dev.* **11:** 786–798.

Fujiwara, K., T.K. Kataoka, and M. Nishizawa. 1993. Two new members of the maf oncogene family, *mafK* and *mafF*, encode nuclear b-Zip proteins lacking putative trans-activator domain. *Oncogene* **8:** 2371–2380.

Hogan, B., R. Beddington, F. Costantini, and E. Lacy. 1994. *Manipulating the mouse embryo.* Cold Spring Harbor Laboratory Press, Cold Spring Harbor, NY.

Igarashi, K., K. Kataoka, K. Itoh, N. Hayashi, M. Nishizawa, and M. Yamamoto. 1994. Regulation of transcription by dimerization of erythroid factor NF-E2 p45 with small Maf proteins. *Nature* **367:** 568–572.

Itoh, K., K. Igarashi, N. Hayashi, M. Nishizawa, and M. Yamamoto. 1995. Cloning and characterization of a novel erythroid cell-derived CNC family transcription factor heterodimerizing with the small Maf family proteins. *Mol. Cell. Biol.* **15:** 4184–4193.

Itoh, K., T. Chiba, S. Takahashi, T. Ishii, K. Igarashi, Y. Katoh, T. Oyake, N. Hayashi, K. Satoh, I. Hatayama, M. Yamamoto, and Y. Nabeshima. 1997. An Nrf2/small Maf heterodimer mediates the induction of phase II detoxifying enzyme genes through antioxidant response elements. *Biochem. Biophys. Res. Comm.* **236:** 313–322.

Jackson, C.W. 1973. Cholinesterase as a possible marker for early cells of the megakaryocytic series. *Blood* **42:** 413–421.

Johnsen, O., N. Skammelsrud, L. Luna, M. Nishizawa, H. Prydz, and A.B. Kolsto. 1996. Small Maf proteins interact with the human transcription factor TCF11/Nrf1/LCR-F1. *Nucleic Acids Res.* **24:** 4289–4297.

Kataoka, K., K.T. Fujiwara, M. Noda, and M. Nishizawa. 1994a. MafB, a new Maf family transcription activator that can associate with Maf and Fos, but not with Jun. *Mol. Cell. Biol.* **14:** 7581–7591.

Kataoka, K., M. Noda, and M. Nishizawa. 1994b. Maf nuclear oncoprotein recognizes sequences related to an AP-1 site and forms heterodimers with both Fos and Jun. *Mol. Cell. Biol.* **14:** 700–712.

Kataoka, K., K. Igarashi, K. Itoh, K.T. Fujiwara, M. Noda, M. Yamamoto, and M. Nishizawa. 1995. Small Maf proteins heterodimerize with Fos and may act as competitive repres-

sors of the NF-E2 transcription factor. *Mol. Cell. Biol.* **15:** 2180–2190.

Kotkow, K.J. and S.H. Orkin. 1996. Complexity of the erythroid transcription factor in NF-E2 as revealed by gene targeting of the mouse p18 NF-E2 locus. *Proc. Natl. Acad. Sci.* **93:** 3514–3518.

Luna, L., O. Johnsen, A.H. Skartlien, F. Pedeutour, C. Turc-Carel, H. Prydz, and A.B. Kolsto. 1994. Molecular cloning of a putative novel human bZIP transcription factor on chromosome 17q22. *Genomics* **22:** 553–562.

Mansour, S.J., K.R. Thomas, and M.R. Capecchi. 1988. Disruption of the protooncogene *int-2* in mouse embryo-derived stem cells: A general strategy for targeting mutations to nonselectable genes. *Nature* **336:** 348–352.

Mohler, J., K. Vani, S. Leung, and A. Epstein. 1991. Segmentally restricted, cephalic expression of a leucine zipper gene during Drosophila embryogenesis. *Mech. Dev.* **34:** 3–9.

Moi, P., K. Chan, I. Asunis, A. Cao, and Y.W. Kan. 1994. Isolation of NF-E2-related factor 2 (Nrf2), a NF-E2-like basic leucine zipper transcriptional activator that binds to the tandem NF-E2/AP1 repeat of the beta-globin locus control region. *Proc. Natl. Acad. Sci.* **91:** 9926–9930.

Motohashi, H., K. Igarashi, K. Onodera, H. Ohtani, M. Nishizawa, J.D. Engel, and M. Yamamoto. 1996. Mesodermal- versus neuronal-specific expression of MafK is regulated by alternative promoters. *Genes Cells* **1:** 223–238.

Motohashi, H., J.A. Shavit, K. Igarashi, M. Yamamoto, and J.D. Engel. 1997. The world according to Maf. *Nucleic Acids Res.* **25:** 2953–2960.

Nagai, T., K. Igarashi, J. Akasaka, K. Furuyama, H. Fujita, N. Hayashi, M. Yamamoto, and S. Sassa. 1998. Regulation of NF-E2 activity in erythroleukemia cell differentiation. *J. Biol. Chem.* **273:** 5358–5365.

Nagy, A. and J. Rossant. 1993. Production of completely ES cell-derived fetuses. In *Gene targeting: A practical approach* (ed. A.L. Joyner), pp. 147-179. IRL Press, Oxford, UK.

Nagy, A., J. Rossant, R. Nagy, N.W. Abramow, and J.C. Roder. 1993. Derivation of completely cell culture-derived mice from early-passage embryonic stem cells. *Proc. Natl. Acad. Sci.* **90:** 8424–8428.

Nishizawa, M., K. Kataoka, N. Goto, K. Fujiwara, and S. Kawai. 1989. v-*maf*, a viral oncogene that encodes a ''leucine zipper'' motif. *Proc. Natl. Acad. Sci.* **86:** 7711–7715.

Oyake, T., K. Itoh, H. Motohashi, N. Hayashi, H. Hoshino, M. Nishizawa, M. Yamamoto, and K. Igarashi. 1996. Bach proteins belong to a novel family of BTB-basic leucine zipper transcription factors that interact with MafK and regulate transcription through the NF-E2 site. *Mol. Cell. Biol.* **16:** 6083–6095.

Ramirez-Solis, R., J. Rivera-Perez, J.D. Wallace, M. Wims, H. Zheng, and A. Bradley. 1992. Genomic DNA microextraction: A method to screen numerous samples. *Anal. Biochem.* **201:** 331–335.

Shivdasani, R.A., M.F. Rosenblatt, D.C. Zucker-Franklin, W. Jackson, P. Hunt, C.J. Saris, and S.H. Orkin. 1995. Transcription factor NF-E2 is required for platelet formation independent of the actions of thrombopoietin/MGDF in megakaryocyte development. *Cell* **81:** 695–701.

Swaroop, A., J. Xu, H. Pawar, A. Jackson, C. Skolnick, and N. Agarwal. 1992. A conserved retina-specific gene encodes a basic motif/leucine zipper protein. *Proc. Natl. Acad. Sci.* **89:** 266–270.

Tybulewicz, V.L., C.E. Crawford, P.K. Jackson, R.T. Bronson, and R.C. Mulligan. 1991. Neonatal lethality and lymphopenia in mice with a homozygous disruption of the c-*abl* protooncogene. *Cell* **65:** 1153–1163.

Wurst, W. and A.L. Joyner. 1993. Production of targeted embryonic stem cell clones. In *Gene targeting: A practical approach* (ed. A.L. Joyner), pp. 33–61. IRL Press, Oxford, UK.